Circulation

ORIGINAL RESEARCH ARTICLE

Flipped C-Terminal Ends of apoA1 Promote ABCA1-Dependent Cholesterol Efflux by Small HDLs

Yi He, PhD; Chiara Pavanello, PhD; Patrick M. Hutchins, PhD; Chongren Tang, PhD; Mohsen Pourmousa, PhD; Tomas Vaisar, PhD; Hyun D. Song, PhD; Richard W. Pastor, PhD; Alan T. Remaley, MD, PhD; Ira J. Goldberg, MD; Tina Costacou, PhD; W. Sean Davidson, PhD; Karin E. Bornfeldt, PhD; Laura Calabresi, PhD; Jere P. Segrest, MD; Jay W. Heinecke, MD

BACKGROUND: Cholesterol efflux capacity (CEC) predicts cardiovascular disease independently of high-density lipoprotein (HDL) cholesterol levels. Isolated small HDL particles are potent promoters of macrophage CEC by the ABCA1 (ATP-binding cassette transporter A1) pathway, but the underlying mechanisms are unclear.

METHODS: We used model system studies of reconstituted HDL and plasma from control and lecithin-cholesterol acyltransferase (LCAT)–deficient subjects to investigate the relationships among the sizes of HDL particles, the structure of apoA1 (apolipoprotein A1) in the different particles, and the CECs of plasma and isolated HDLs.

RESULTS: We quantified macrophage and ABCA1 CEC of 4 distinct sizes of reconstituted HDL. CEC increased as particle size decreased. Tandem mass spectrometry analysis of chemically cross-linked peptides and molecular dynamics simulations of apoA1, the major protein of HDL, indicated that the mobility of C-terminus of that protein was markedly higher and flipped off the surface in the smallest particles. To explore the physiological relevance of the model system studies, we isolated HDL from LCAT-deficient subjects, the small HDLs (eg, reconstituted HDLs) of which are discoidal and composed of apoA1, cholesterol, and phospholipid. Despite their very low plasma levels of HDL particles, these subjects had normal CEC. In both the LCAT-deficient subjects and control subjects, the CEC of isolated extra-small HDL (a mixture of extra-small and small HDL by calibrated ion mobility analysis) was 3- to 5-fold greater than that of the larger sizes of isolated HDL. Incubating LCAT-deficient plasma and control plasma with human LCAT converted extra-small and small HDL particles into larger particles, and it markedly inhibited CEC.

CONCLUSIONS: We present a mechanism for the enhanced CEC of small HDLs. In smaller particles, the C-termini of the 2 antiparallel molecules of apoA1 are "flipped" off the lipid surface of HDL. This extended conformation allows them to engage with ABCA1. In contrast, the C-termini of larger HDLs are unable to interact productively with ABCA1 because they form a helical bundle that strongly adheres to the lipid on the particle. Enhanced CEC, as seen with the smaller particles, predicts decreased cardiovascular disease risk. Thus, extra-small and small HDLs may be key mediators and indicators of the cardioprotective effects of HDL.

Key Words: ABCA1 ■ chemical cross-linking ■ cholesterol efflux capacity ■ molecular dynamics simulation ■ peptide analysis

The risk of cardiovascular disease (CVD) strongly and inversely associates with plasma levels of high-density lipoprotein cholesterol (HDL-C).[1] However, pharmacological interventions that elevate HDL-C have failed to lower CVD risk in statin-treated subjects, suggesting that the association between HDL-C and CVD

Correspondence to: Jay W. Heinecke, MD, 850 Republican St, Box 358055, UW Medicine, Seattle, WA 98109. Email heinecke@uw.edu
Supplemental Material is available at https://www.ahajournals.org/doi/suppl/10.1161/CIRCULATIONAHA.123.065959.
For Sources of Funding and Disclosures, see page XXX.

Circulation is available at www.ahajournals.org/journal/circ

Clinical Perspective

What Is New?

- Using chemical cross-linking and molecular dynamics simulations, we showed that the C-termini of apoA1 (apolipoprotein A1), the major protein of high-density lipoprotein (HDL), have increased mobility and conformational freedom in small HDL particles.
- The enhanced mobility of the C-termini of apoA1 in small HDLs allows the C-termini to "flip" off the surface of a particle, activating ABCA1 (ATP-binding cassette transporter A1), thereby stimulating cholesterol removal from cells.
- Because of the vital role of small HDL in cholesterol efflux, quantification of HDL particle concentration determined by calibrated ion mobility analysis (the size and concentration of HDL subspecies) might be a better metric for gauging cardiovascular disease risk than HDL cholesterol levels.
- Therapeutic interventions that increase small HDL levels, with or without increasing HDL cholesterol levels, may be cardioprotective.

Nonstandard Abbreviations and Acronyms

ABCA1	ATP-binding cassette transporter A1
apoA1	apolipoprotein A1
apoB	apolipoprotein B
CEC	cholesterol efflux capacity
CVD	cardiovascular disease
EDC	1-ethyl-3-(3-dimethylaminopropyl) carbodiimide hydrochloride
HDL	high-density lipoprotein
HDL-C	high-density lipoprotein cholesterol
IMA	ion mobility analysis
LCAT	lecithin-cholesterol acyltransferase
L-HDL	large HDL
MD	molecular dynamics
M-HDL	medium HDL
r-HDL	reconstituted HDL
S-HDL	small HDL
XS-HDL	extra-small HDL

risk is indirect.[2] It is therefore critical to identify new mechanisms that inversely link high-density lipoprotein (HDL) to CVD risk and do not involve HDL-C.[3,4]

One proposed cardioprotective function of HDL is promotion of cholesterol efflux from lipid-laden macrophages, which play critical roles in all stages of atherogenesis.[5] Two early steps in this pathway involve ATP-binding cassette transporters, ABCA1 and ABCG1. Initially, ABCA1 mediates cholesterol efflux from macrophages to lipid-poor apolipoproteins[6] and small, dense HDL.[7,8] Lecithin-cholesterol acyltransferase (LCAT) then promotes HDL maturation by catalyzing the conversion of free cholesterol to cholesteryl esters, which are then transferred from the surface to the core, generating larger HDL particles.[9] ABCG1 exports cellular cholesterol to larger HDL particles that deliver cholesterol to the liver for excretion in bile.[2]

Rothblat et al demonstrated that serum HDL (serum depleted of lipoproteins that contain apoB [apolipoprotein B]) promotes cholesterol efflux from cultured macrophages, thus mimicking the key early steps in reverse cholesterol transport from macrophages.[10,11] The magnitude of cholesterol efflux to serum HDL, termed cholesterol efflux capacity (CEC), is largely independent of HDL-C.[10,11] However, large clinical studies demonstrate that macrophage CEC and ABCA1-specific CEC of serum HDL strongly and negatively associate with prevalent and incident CVD.[12] It is important to note that CEC predicts CVD independently of HDL-C.[11–13] These results suggest that CEC is a critical contributor to the proposed antiatherogenic functions of HDL in humans.

LCAT is widely regarded as an important driving force for mobilizing cholesterol from tissues to the liver for excretion. However, subjects with complete LCAT deficiency do not appear to be at increased risk for CVD[14] despite having very low HDL-C levels. Animal models of atherosclerosis have yielded conflicting results on the impact of LCAT deficiency and overexpression.[15,16] Serum from LCAT-deficient subjects exhibits elevated ABCA1-dependent cellular cholesterol efflux although efflux by ABCG1 and SR-B1 is impaired, suggesting that cholesterol efflux by the ABCA1 pathway might explain why those subjects are not at high risk for CVD.[17]

CSL-112, a reconstituted HDL (r-HDL) particle composed of human apoA1 (apolipoprotein A1) and phosphatidylcholine, was designed to mimic small HDLs (S-HDLs).[18] The drug, which markedly enhances the ABCA1 CEC of human plasma, promotes the remodeling of HDL, resulting in higher levels of small and lipid-poor apoA1 particles.[19]

S-HDLs account for most of the CEC activity of serum HDL.[7,8] However, the underlying mechanisms are poorly understood. To explore potential mechanisms, we combined functional and structural studies of r-HDL particles with studies of control and LCAT-deficient subjects. Our studies reveal that the C-terminus of apoA1 in smaller HDLs becomes available to engage ABCA1, the first key step in cholesterol export from cells.

METHODS

Generation of r-HDL Particles

Discoidal r-HDL was prepared from recombinant human apoA1, 1-palmitoyl-oleoyl-phosphatidylcholine, and free cholesterol by cholate dialysis.[20–22] The composition of the different

size of particles is: (apoA1:free cholesterol:1-palmitoyl-oleoyl-phosphatidylcholine, mol/mol): r-HDL-80, 1.0:1.8:34; r-HDL-88, 1.0:2.9:52.7; r-HDL-96, 1.0:4.7:90.6; r-HDL-120, 1.0:4.7:140.[22]

Calibrated Ion Mobility Analysis

The sizes of r-HDL and human HDL particles were quantified with a scanning mobility particle sizer spectrometer (TSI Inc, Shoreview, MN, model 3080N).[23–25] The concentrations of r-HDL and HDL particles (moles per liter) were determined using a calibration curve of glucose oxidase.[23]

Chemical Cross-Linking of r-HDL

r-HDLs were cross-linked with 1-ethyl-(3-dimethylaminopropyl) carbodiimide hydrochloride (EDC) in phosphate-buffered saline (pH 6.5)[20,26] and further fractionated by high-resolution size exclusion chromatography to isolate monomeric HDL particles. Details are provided in the Supplemental Material.

Proteolytic Digestion and Mass Spectrometry Analysis

Details are provided in the Supplemental Material.

Molecular Dynamics Simulations of r-HDL

Molecular dynamics (MD) trajectories of r-HDL-80 and r-HDL-90 were calculated using a combination of all-atom simulation, simulated tempering, and coarse-grained methods (Supplemental Material).[27–30] Simulations of r-HDL-100 and r-HDL-120 (termed r-HDL-110) were reported previously.[27] Because different preparations of the largest r-HDL particles range in size from 110 to 120 Å,[22] we term these r-HDL-120 to be consistent with the size of the largest particles used here.

HDL Contact Map Analyses

Inter- and intramolecular contact maps between Cα atoms used a cutoff distance of 15.1 Å.[27] A total of 2084 and 1042 frames from the last half of 20-μs and 10-μs simulations were used for the r-HDL-100 and r-HDL-120 particles, respectively.[27] A total of 100 frames extracted from the last half of 200-μs coarse-grained simulations of r-HDL-80 and r-HDL-90 particles were converted to all-atom structures to develop the contact maps. Contact maps were plotted using Gnuplot version 5.2 (http://gnuplot.info).

Cholesterol Efflux Capacity

Macrophage CEC was assessed with J774 macrophages labeled with [^{3}H]cholesterol and stimulated with a cAMP analog.[10] Efflux by the ABCA1 pathway was measured with baby hamster kidney cells that expressed mifepristone-inducible human ABCA1 and were labeled with [^{3}H]cholesterol.[6]

LCAT-Deficient and Control Subjects

Twenty-four subjects (4 carriers of 2 mutant LCAT alleles [termed LCAT-/- subjects], 6 carriers of one mutant LCAT allele [LCAT+/-], and 14 noncarriers [LCAT+/+]) were from an Italian family study. The Italian LCAT deficient cohort includes related carriers (Table S1).[31] Two additional LCAT-/- subjects were from New York. The study was approved by the institutional review boards of Milano Area C, Italy (446-092014), New York University (I14-01537), and the University of Washington (STUDY00012123). All subjects gave informed consent. Aliquots of serum from subjects who had fasted overnight were immediately frozen and stored at −80 °C until analysis. Serum lipid levels and LCAT activity of the Italian cohort were determined as described.[31]

Incubation of Control and LCAT-Deficient Plasma With LCAT

Details are provided in the Supplemental Material.[32]

HDL Isolation

For functional studies, HDL was first isolated by ultracentrifugation (density, 1.063–1.210 g/mL)[33] from serum of control subjects (n=4) and LCAT-/- subjects (n=5) and then fractionated on a Superdex 200 Increase 10/300 GL column. Details are provided in the Supplemental Material.

Data Availability

All data supporting the findings of this study are available in the article or its Supplemental Material.

Statistical Analyses

Statistical analyses were performed with STATA software version 12 (Stata Corp, College Park, TX) and with SAS v.9.4 (SAS Inc, Cary, NC). Mixed-effect models, considering family as a random effect, with Tukey-Kramer post hoc tests were used to compare the means of 3 or more groups. One-way ANOVA was used to analyze laboratory experiments. Linear regression was used to investigate the correlation of serum HDL CEC with HDL particle concentration for each subspecies. Parametric or nonparametric analyses were based on the Shapiro-Wilk test for normality. The ratio *t* test (GraphPad) was used for the analysis of plasma incubations with or without LCAT. The null hypothesis is that the average of the logarithms of the ratio of each pair is 0. *P* values <0.05 were considered significant. Unless otherwise stated, values represent means±SDs.

RESULTS

Reconstituted S-HDL Particles Promote Macrophage CEC and ABCA1 CEC as Effectively as Lipid-Free apoA1

We used discoidal r-HDL as a model system to investigate how particle size affects the ability of HDL to promote CEC.[20,22] To quantify cholesterol efflux by macrophages and the ABCA1 pathway, we used validated model systems.[8,10,11] r-HDLs were fractionated into 4 different sizes of particles, using high-resolution size exclusion chromatography.[20] We term these particles r-HDL-80, r-HDL-88, r-HDL-96, and r-HDL-120

because their diameters are respectively 80 Å, 88 Å, 96 Å, and 110 to 120 Å as determined by calibrated ion mobility analysis (IMA; Figure 1A). These values are in excellent agreement with those previously determined by non-denaturing gradient gel electrophoresis and by quantification of the hydrodynamic Stokes' diameters of the particles.[22]

Each particle population exhibited a symmetrical Gaussian-like distribution and was clearly distinguishable from the other sizes of particles by IMA (Figure 1A). The r-HDL particles were similar in size to human extra-small HDL (XS-HDL), S-HDL, medium HDL (M-HDL), and large HDL (L-HDL) (see below).

At equimolar concentrations, the smallest r-HDL-80 particles were as effective as lipid-free apoA1 at promoting both macrophage CEC and ABCA1 CEC (Figure 1B). The r-HDL-88 particles were less effective, and the 2 largest r-HDL particles (r-HDL-96 and r-HDL-120) failed to promote either macrophage CEC or ABCA1 CEC.

Probing the Structure of apoA1 in r-HDLs With Tandem Mass Spectrometry

In their double-belt model for HDL, Segrest et al[34] proposed that 2 molecules of apoA1 form an antiparallel helical bundle that encircles the edge of the discoidal HDL particle. The crystal structure of N-terminally truncated apoA1[35] and chemical cross-linking studies of r-HDL[20,27,36] and human HDL[20] support this model.

In contrast with the central region of apoA1, which forms a stable helical bundle, the N-terminal and C-terminal regions of apoA1 in HDL are more flexible and capable of assuming a variety of conformations.[22,27,36,37] These regions of the protein are also important for promoting ABCA1-dependent cholesterol efflux.[36] To investigate the structures of the different regions of apoA1 in the different sizes of r-HDL, we used EDC[20] to generate intramolecular and intermolecular 0-order cross-links in apoA1. EDC reacts with the amino group of lysine residues that are close to the carboxylic acid group of aspartate and glutamate to form an amide bond. Thus, EDC cross-links identify salt bridges in structures. The cross-linked r-HDLs were reisolated by high-resolution size exclusion chromatography to eliminate HDL particles that were cross-linked to each other. It is important to note that all cross-linking reactions were carried out at low concentrations of EDC in phosphate-buffered normal saline at pH 6.5, which more closely mimics physiological conditions than those used to crystallize proteins.

After the cross-linked apoA1 was digested, the resulting peptide mixture was fractionated by capillary liquid chromatography and analyzed by tandem mass spectrometry. To distinguish between inter- and intramolecular cross-links of apoA1 in r-HDL, we used a 1:1 mixture of human [^{14}N]apoA1 (light, L) and [^{15}N]apoA1 (heavy, H) (isotopic purity >99%) to generate the particles.[20,38] Three combinations of cross-links are possible: L-L, L-H, and H-H. The L and H forms of apoA1 are chemically identical but differ in molecular mass, making intramolecular and intermolecular cross-links readily distinguishable in MS1 scans. For intraprotein cross-links, in which the protein is linked to itself, only L-L and H-H forms are detected (relative abundance ≈1:1). For interprotein cross-links, L-L, L-H, and H-H peptides are detected (relative abundance ≈1:2:1; Figure S1 and S2).[20,38]

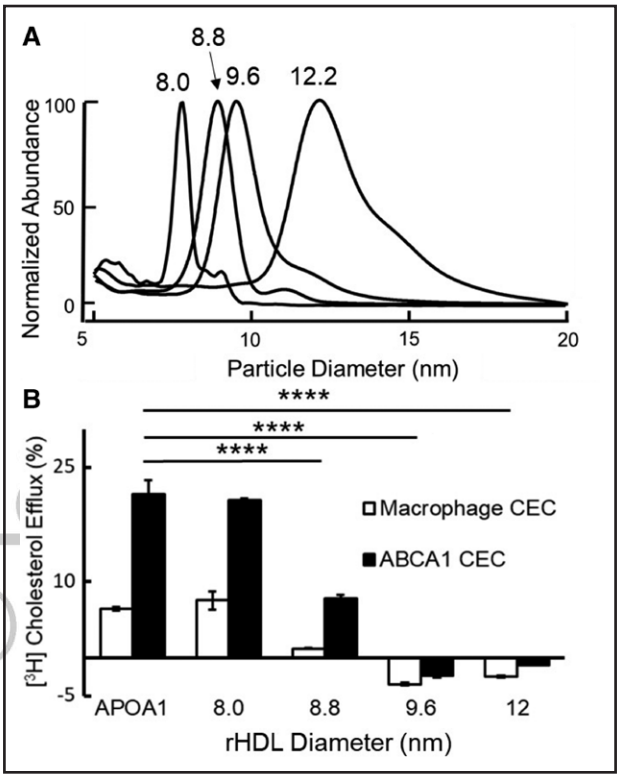

Figure 1. Calibrated IMA (A) and CEC (B) of reconstituted HDLs (r-HDLs) prepared by cholate dialysis and fractionation by high-resolution size exclusion chromatography.
A, Representative IMA profiles of each size of r-HDL. To facilitate comparison of the size distributions of the particles, the height of each r-HDL was set to 100%. The median sizes of the isolated particles were 8.0±0.2 nm, 8.8±0.1 nm, 9.6±0.1 nm, and 12.2±0.1 nm. **B**, ABCA1-mediated CEC using equimolar concentrations of each size of r-HDL. Macrophage CEC and ABCA1 CEC of serum HDL were quantified after a 4-hour incubation with [^{3}H]cholesterol-labeled J774 macrophages and baby hamster kidney cells, without or with induction of ABCA1 expression with cAMP and mifepristone, respectively. Cholesterol efflux was calculated as the percentage of radiolabel in the medium of the cells divided by the total radioactivity of the medium and cells. CEC was quantified as the difference in cholesterol efflux of cells with and without induced expression of ABCA1. Results are representative of 5 independent experiments with replicate analyses. ****P<0.001, 1-way ANOVA with Tukey-Kramer post-tests. ABCA1 indicates ATP-binding cassette transporter A1; apoA1, apolipoprotein A1; CEC, cholesterol efflux capacity; HDL, high-density lipoprotein; and IMA, ion mobility analysis.

Different Sizes of r-HDL Exhibit Distinct Patterns of Intramolecular and Intermolecular Cross-Links Between Peptides in the N-Terminal and C-Terminal Regions of apoA1

This approach identified 34 intramolecular and 31 intermolecular cross-links in the 4 sizes of r-HDL (Table S2). Similar numbers of intramolecular cross-links were detected in the 3 largest particles (r-HDL-120, 8 cross-links; r-HDL-96, 6 cross-links; r-HDL-88, 7 cross-links). In contrast, we identified twice as many intramolecular cross-links in the r-HDL-80 particle (13 cross-links). These observations indicate that apoA1 has greater conformational freedom in the smallest r-HDL particles than in the other sizes of HDL.

Probing the Behavior of HDL Particles Over Time With MD Simulations

To investigate how apoA1 conformation and mobility vary in the different sizes of r-HDL, we used a computational method called MD. Here trajectories of systems modeling r-HDL (2 apoA1 bound to a nanodisc composed of 1-palmitoyl-oleoyl-phosphatidylcholine and ≈10% cholesterol, and surrounded by water) are generated for multiple microseconds. The result is a series of snapshots of the dynamic evolution for all of the atoms in the system.

We previously used this approach to generate trajectories of r-HDL-100 and r-HDL-120 particles (100 Å and 120 Å diameter particles [Supplemental Material]).[27] To generate the double-belt models for r-HDL-80 and r-HDL-90 particles (80 Å and 90 Å diameter particles), we ran MD simulations after removing cholesterol and 1-palmitoyl-oleoyl-phosphatidylcholine from the computer-generated r-HDL-100 particle (Supplemental Material). We then determined whether the cross-links we identified in apoA1 in the different sizes of r-HDL were consistent with the double-belt model.[34]

To perform this analysis, we compared intermolecular and intramolecular distances between Cα atoms in the models using an HDL contact map to plot a detected peptide by the position of its 2 amino acids in the sequence of apoA. The maximum distance between the backbone Cα atoms of amino acids in the cross-linked peptides is the sum of the length of 2 side chains plus the length of the amide bond formed by EDC (10.5 Å for K–D linkage and 12.1 Å for K–E). Figure 2 shows the position of each cross-link in the contact maps for the simulated belt structure for each size of HDL. The cutoff radius for the cross-link residing in the double-belt model was 15.1 Å (12.1 Å for the K–D cross-link plus a 3 Å motion averaging factor).[27]

Only 1 of the cross-links detected in the largest particle (r-HDL-120) was inconsistent with the double-belt model of HDL (Figure 2A; intermolecular cross-links, red regions; intramolecular cross-links, green regions). Just 2 of the cross-links in the r-HDL-100 particle were inconsistent (Figure 2B). In contrast, 7 and 9 cross-links in the r-HDL-90 and r-HDL-80 particles were inconsistent with the prototypical double-belt model. In r-HDL-90, 4 of the 7 cross-links were in the C-terminus of apoA1; in r-HDL-80, 6 of the 9 cross-links were in the C-terminus (Figure 2C and 2D). The large number of cross-links in the C-terminus of the 2 smallest particles (r-HDL-90 and r-HDL-80) indicates that this region is more loosely organized than in the larger particles and thus underwent a larger number of cross-linking reactions in the experiment.

These observations indicate that the central region of the apoA1 dimer is organized as a double belt in all the sizes of r-HDL we studied. In contrast, the N-terminal and C-terminal regions differ according to particle size. Specifically, the C-termini of apoA1 are markedly more mobile in the 2 smallest particles. Many of the observed cross-links in the N-termini of apoA1 of the 3 smallest HDLs also fell outside the contact zones predicted by the double-belt model (Figure 2B through 2D), which is consistent with the proposal that the N-terminus apoA1 in r-HDL-100 is hinged.[27]

The C-Termini of S-HDL Particles Exhibit Freater Mobility Than Those of L-HDL Particles

Figure 3A through 3H illustrates the conformational states of apoA1 obtained by MD simulations of the HDL particles of varying sizes, with lipids and water excluded from the image for clarity. In the case of r-HDL-120 particles, the 2 proteins adopt a predominantly double-belt arrangement, although some displacement of the C-terminal helices (H10A and H10B) occurs.[27] Disorder in the N-terminal region (residues 1–43) is noticeable in r-HDL-100 particles, and both the N-termini and C-termini lose their double-belt characteristics in r-HDL-90 particles. Both C-termini are flipped off the lipid edge in the r-HDL-90 particles (Figure 3E and 3F).

The structure of the smallest particle, r-HDL-80, markedly differs from that of the larger r-HDL particles. The smallest particles are shaped like a spherical micelle, deviating from the disk-like structure, and the double-belt arrangement is largely absent except for helix 5 (green; Figure 3G and 3H). There is also significant unwinding and displacement of the C-terminal helices.

It is important to note that the images (Figure 3) represent snapshots of individual simulations at specific time points and do not capture the complete flexibility of the terminal helices. Although the simulations of the large r-HDL-100 and r-HDL-120 particles show that the C-termini remain associated with the lipid surface, they could detach in the presence of a protein such as ABCA1. Thus, these images represent low-energy states but not the sole states achievable by these systems.[28] It

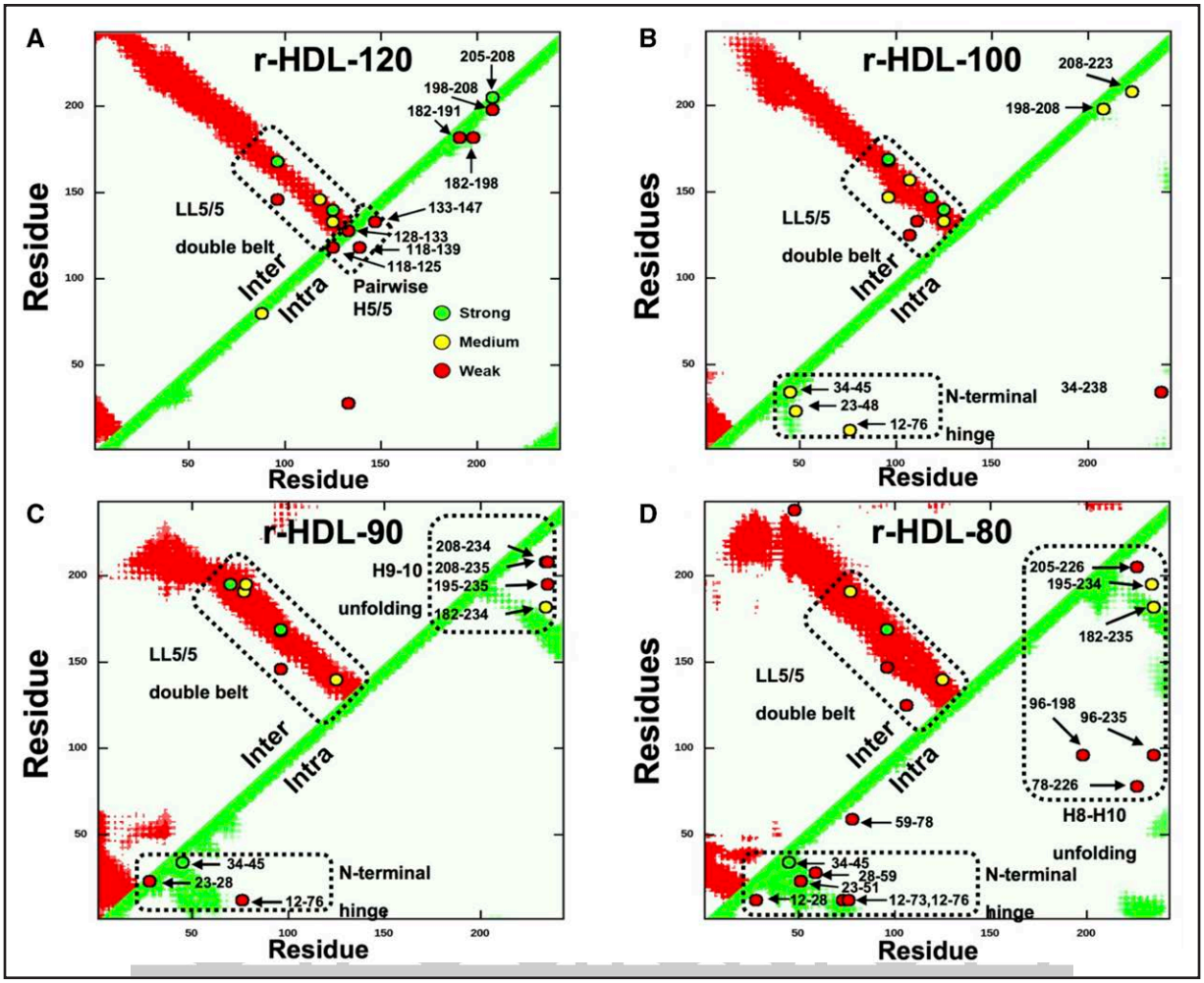

Figure 2. Contact maps of the intermolecular (Inter) and intramolecular (Intra) apoA1 (apolipoprotein A1) cross-links detected by tandem mass spectrometry (MS/MS) in different sizes of r-HDL.
Red regions and green regions indicate the allowable distance of intermolecular and intramolecular peptide contacts (15.1 Å), respectively, in a molecular dynamics simulation of the LL5/5 double-belt model of apoA1.[27] Cross-links (o) between apoA1 residues are labeled. Semiquantitative estimates of the strengths of interactions between residues were based on ion currents (Table S2), and they are indicated by the colors of the circles (green, strong; yellow, medium; and red, weak). Note that we detected multiple intramolecular cross-linked peptides in the helix 8 to helix 10 region and the helix 9 to helix 10 region of the C-terminus of apoA1 of r-HDL-80 and r-HDL-90 particles, respectively, that are inconsistent with the classic double-belt model. This indicates that the C-terminus of apoA1 has increased conformational freedom and does not assume the double-belt conformation in that region. In contrast, the intramolecular cross-linked peptides detected in that region of the 2 largest sizes of high-density lipoprotein are consistent with the double-belt model. r-HDL indicates reconstituted high-density lipoprotein.

is also worth noting that the time scale, potential energy functions, and restraints employed in the all-atom and coarse-grained simulations tend to maintain the helical structure of the protein residues.

Clinical Characteristics of LCAT-Deficient and Control Subjects

Like the r-HDL particles used in our model system studies, the XS-HDL and S-HDL particles in LCAT-deficient subjects are discoidal and composed largely of apoA1, free cholesterol, and phospholipid.[39,40] We therefore used serum HDL and HDLs isolated from control and LCAT-deficient subjects to investigate the relevance of our model system studies to human HDL.

We studied 3 groups of subjects: 14 controls, 6 subjects with heterozygous LCAT deficiency (LCAT+/-), and 6 with LCAT deficiency (LCAT-/-).[31] Two of the LCAT-/- subjects were unrelated to the subjects in the family study. The 3 groups had similar ages, percentages of females, and plasma low-density lipoprotein cholesterol levels (Table). Compared with the LCAT+/+ subjects, the LCAT$^{+/-}$ subjects had significantly lower plasma HDL-C levels, as did the LCAT-/- subjects (P=0.0005). Plasma triglyceride levels were not significantly different between the groups (P=0.28; mixed-effect model and Tukey-Kramer post-tests). LCAT activity was undetectable in the LCAT-/- subjects (0 nmol/mL per h), with significantly higher levels in the LCAT+/- subjects and LCAT+/+ subjects (P<0.0001).

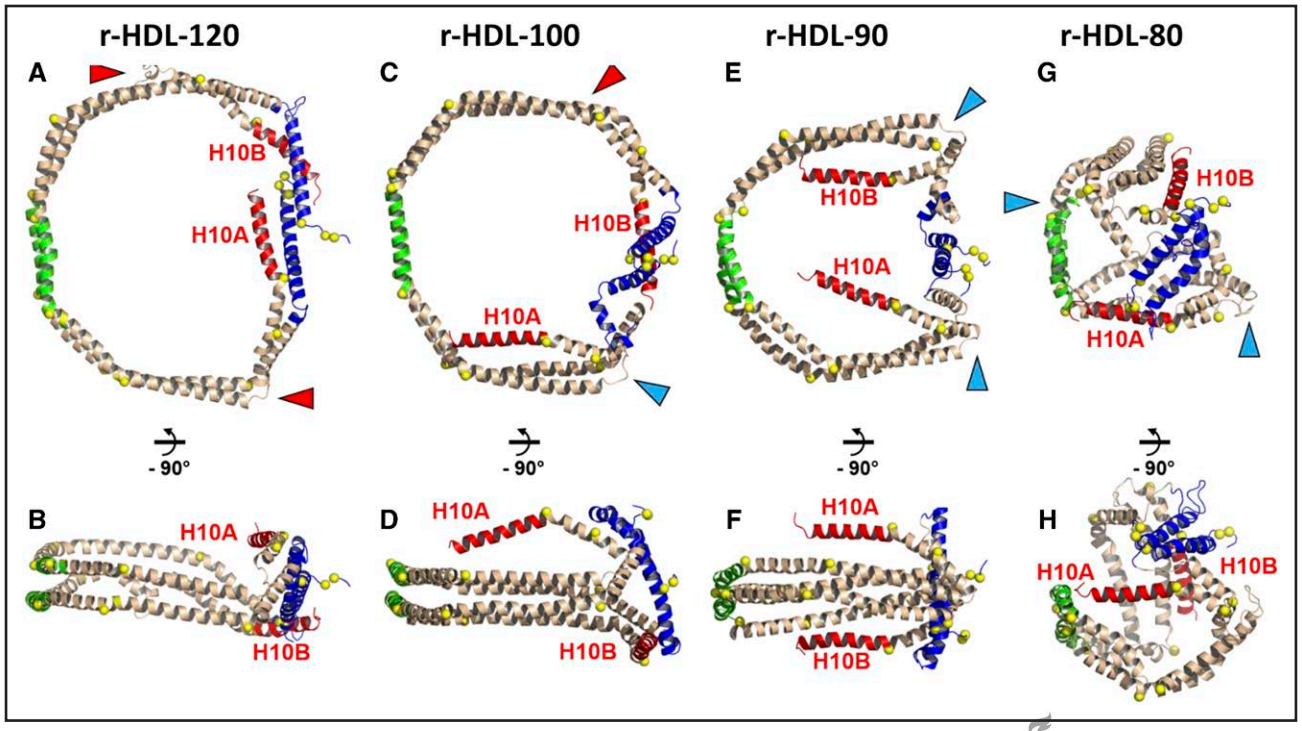

Figure 3. Comparison of stepwise conformational changes in apoA1 (apolipoprotein A1) between r-HDL-120, r-HDL-100, r-HDL-90, and r-HDL-80 particles.

Animatated representations: blue, N-terminal 43 (residues 1–43); green, pairwise helix 5 (residues 121–143); red, helix 10 (residues 220–243). Red arrowheads show the partially unfolded H7-H8 junctions. Blue arrowheads show the hairpin coil that allows helix 10 (H10A and H10B) to fold onto the 1-palmitoyl-oleoyl-phosphatidylcholine headgroup surface. **A**, Top view of r-HDL-120. **B**, Side view of r-HDL-120. **C**, Top view of r-HDL-100. **D**, Side view of r-HDL-100. **E**, Top view of r-HDL-90. **F**, Side view of r-HDL-90. **G**, Top view of r-HDL-80. **H**, Side view of r-HDL-80. Note that apoA1 in the 2 largest HDL particles (**A** through **D**; r-HDL-120 and r-HDL-100) has a conformation that is strongly lipid-associated and consistent with the classic double-belt model. In contrast, this structure is absent in both C-termini (H10A and H10B) of apoA1 in the 2 smallest HDL particles (**E** through **H**; r-HDL-90 and r-HDL-80). r-HDL indicates reconstituted high-density lipoprotein.

XS-HDL and S-HDL Particles Are Enriched in LCAT-Deficient Subjects

We used calibrated IMA to quantify total HDL and 4 sizes of HDL particles: XS-HDL, S-HDL, M-HDL, and L-HDL (Figure 4A; Table S3). This method for quantifying HDL particle concentration determined by calibrated IMA yields a stoichiometry of apoA1 and sizes and relative abundances of HDL subspecies that agree well with those determined by nondenaturing gradient gel electrophoresis and analytical ultracentrifugation.[23,41] In the LCAT$^{+/+}$ subjects, M-HDL (mean diameter, 9.2±0.1 nm) was the most abundant particle population; it accounted for ≈50% of total HDL (Figure 4A). All 4 sizes of HDL were detected in all the control subjects. In contrast, subjects with partial LCAT deficiency had elevated levels of XS-HDL (mean diameter, 7.8±0.1 nm) and S-HDL (mean diameter, 8.4±0.1 nm diameter) particles (Figure 4A). Subjects with complete LCAT deficiency exhibited only XS-HDL (Figure 4A).

The total concentration of HDL particles and the distribution of the different sizes of HDL also differed significantly among the 3 groups (Figure 4B through 4; Table S3). Mean total HDL particle concentration levels determined by calibrated IMA in control subjects were 5.1× higher than those in LCAT-/- subjects and 1.8× higher than those in LCAT+/- subjects (P<0.0001). This reflected significantly lower levels of both M-HDL and L-HDL in subjects with complete or partial LCAT deficiency (P<0.0001 for both M-HDL and L-HDL). In contrast, mean levels of XS-HDL were higher in both LCAT-/- and LCAT+/- subjects than in control subjects. LCAT-/- and LCAT+/- subjects had similar levels of XS-HDL and L-HDL.

Serum HDL From LCAT-Deficient Subjects Has Normal Macrophage and ABCA1 CEC Despite Low Total HDL Particle Concentration Determined by Calibrated IMA

We used serum HDL (apoB-depleted serum) to quantify the subjects' CEC, as described by Rothblat et al.[10,11] Macrophage and ABCA1 CEC were evaluated using J774 macrophages stimulated with cAMP or baby hamster kidney cells with mifepristone-inducible expression of human ABCA1. CEC, quantified as the difference in cholesterol efflux with and without induction of ABCA1, was a linear function of serum HDL concentration and incubation time. A mixed-effect model demonstrated that

Table. Clinical Characteristics of the Subjects in the Family Study

Characteristic	Controls (LCAT+/+) n=14	Heterozygotes (LCAT+/-) n=6	Homozygotes (LCAT-/-) n=4	*P* value
Age (y)	49±20	54±16	47±18	0.81
Female/male (n)	5/9	2/4	4/2	…
HDL-C (mg/dL)	71±9	40±11	9.2±6.1	0.0005
LDL-C (mg/dL)	114±32	109±34	111±74	0.22
Triglycerides (mg/dL)	111±61	121±30	253±130	0.28
LCAT activity (nmol/mL per h)	42±9	20±13	0±0	<0.0001

P values are from a mixed-effect model and Tukey-Kramer post-tests. HDL-C indicates high-density lipoprotein cholesterol; LCAT, lecithin-cholesterol acyltransferase; and LDL-C, low-density lipoprotein cholesterol.

macrophage CEC and ABCA1 CEC did not differ significantly between LCAT-/- and control subjects (*P*>0.3).

To begin to identify the HDL subpopulations that drive macrophage CEC and ABCA1 CEC, we correlated the CEC of serum HDL with the particle concentration of each HDL subpopulation from all the study subjects (Figure S3). Macrophage CEC only correlated positively and strongly with the concentration of XS-HDL particle concentration (r=0.55; *P*=0.004). These observations suggest that XS-HDL is an important driver of cellular cholesterol export from both macrophages and through the ABCA1 pathway.

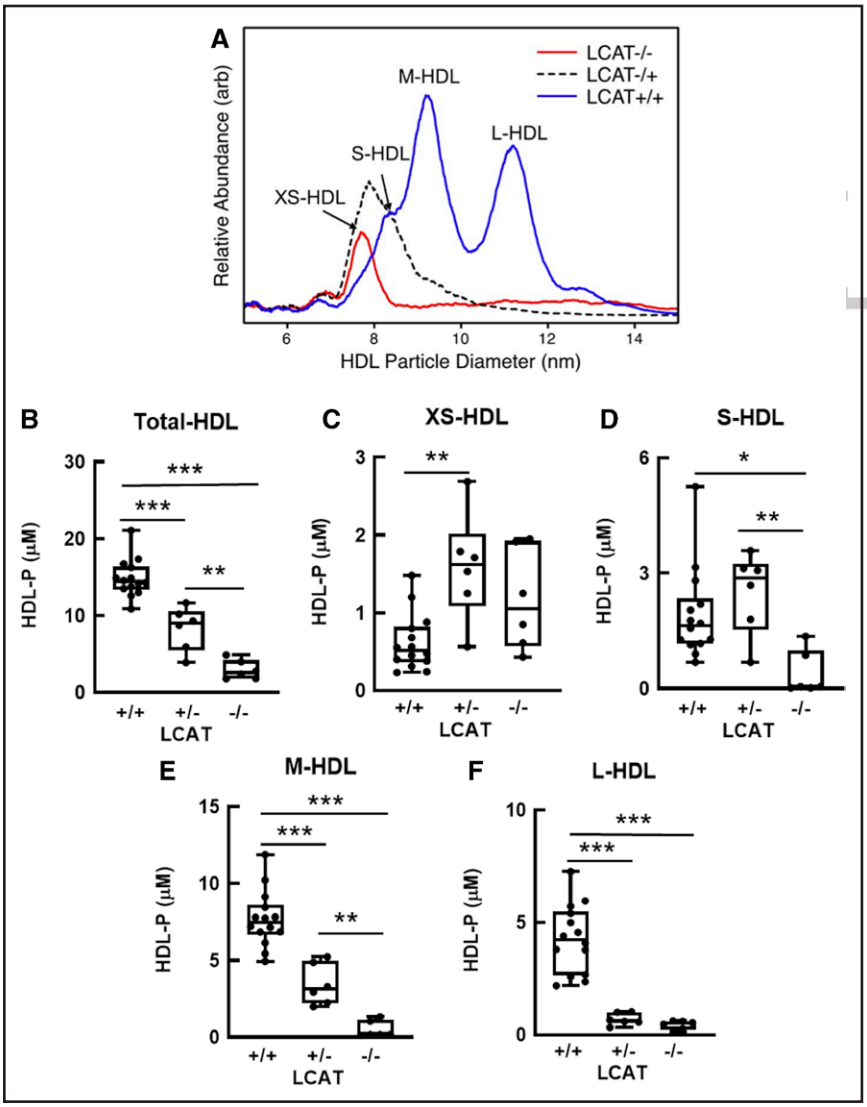

Figure 4. Quantification of total HDL and HDL subspecies in LCAT-deficient (-/-), LCAT-heterozygous (+/-), and control (+/+) subjects.
A, Representative size and concentration profiles of HDL isolated from LCAT-deficient (-/-), LCAT-heterozygous (+/-), and control (LCAT+/+) subjects. **B** through **F**, HDL isolated by ultracentrifugation from plasma (d=1.063–1.21 g/mL) was analyzed by calibrated IMA. The mean HDL subspecies sizes were as follows: extra-small HDL (XS-HDL), 7.8 nm; small HDL (S-HDL), 8.4 nm; medium HDL (M-HDL), 9.2 nm; and large HDL (L-HDL), 10.9 nm. HDL isolated from plasma by ultracentrifugation was subjected to calibrated IMA. The sizes (mean, SD) of the HDL subspecies were as follows: XS-HDL, 7.8±0.1 nm; S-HDL, 8.4±0.1 nm; M-HDL, 9.2±0.1 nm; and L-HDL, 10.9±0.2 nm. The number of subjects was as follows: LCAT+/+, n=14; LCAT+/-, n=6; and LCAT-/-, n=6. *P* value, 1-way ANOVA with Tukey-Kramer post-tests. ***$P<0.001$, **$P<0.01$, and *$P<0.05$. arb indicates arbitrary units; HDL, high-density lipoprotein; HDL-P, HDL particle concentration determined by calibrated IMA; IMA, ion mobility analysis; and LCAT, lecithin-cholesterol acyltransferase.

S-HDL and XS-HDL Particles Are the Major Promoters of Macrophage CEC and ABCA1 CEC in Both LCAT-Deficient Subjects and Control Subjects

To further investigate how XS-HDL promotes CEC, we used ultracentrifugation and high-resolution size exclusion chromatography to isolate XS-HDL from LCAT-/- subjects. We then compared the CEC activity of XS-HDL with that of 4 sizes of HDL isolated from LCAT+/+ subjects. The mean diameters of the isolated HDLs were 8.4 nm, 8.8 nm, 9.2 nm, and 14 nm (Figure 5A; size distributions), respectively.

We quantified macrophage and ABCA1 CEC as described above for serum HDL. It is important to note that we incubated the cells with equimolar concentrations of isolated particles of each size of HDL. CEC was a linear function of HDL particle concentration and the incubation time used in the assays. XS-HDL isolated from LCAT-/- subjects, composed almost exclusively of 7.8-nm-diameter particles (XS-HDL–sized), strongly promoted both macrophage and ABCA1 CEC. However, it was less potent than 8.4-nm XS-HDL particles isolated from LCAT+/+ subjects (Figure 5B), which were composed of approximately equimolar amounts of XS-HDL and S-HDL (as determined by calibrated IMA). On a molar basis, 8.4-nm HDL isolated from control subjects was as effective as lipid-free apoA1 in promoting both macrophage CEC and ABCA1 CEC. On a molar basis, XS-HDL isolated from LCAT-/- subjects promoted macrophage CEC much more effectively than 8.8-nm HDL, 9.2-nm HDL, or 14-nm HDL isolated from control subjects, and the differences were significant (P=0.0002 for 8.8-nm HDL, P<0.0001 for 9.2-nm HDL, and P<0.0001 for 14-nm HDL). We obtained similar results when we determined how effectively the different sizes of isolated HDL promoted ABCA1 CEC (Figure 5C).

LCAT Converts S-HDLs Into L-HDLs, Markedly Reducing CEC

To test the hypothesis that LCAT is an important factor controlling the CEC of circulating HDL, we incubated control plasma and LCAT-deficient plasma with or without recombinant human LCAT at 37 °C for 2 h, stopped the LCAT reaction with DTNB, and quantified ABCA1 CEC and HDL particle concentration, using calibrated IMA. Control experiments demonstrated that DTNB had no impact on quantification of ABCA1 CEC.

Before incubation with LCAT, the major HDL species in the LCAT-/- subjects was XS-HDL. In contrast, all 4 sizes of HDL were observed in the control subjects; M-HDL was the most abundant species. LCAT treatment decreased the ABCA1 CEC of both control plasma and LCAT-/- plasma by ≈50% (Figure 6A). LCAT converted virtually all XS-HDL and most S-HDL particles into larger HDLs in plasma of both control and LCAT-deficient subjects (Figure 6B). In plasma treated with LCAT, free cholesterol markedly decreased, whereas total cholesterol did not change significantly (Figure 6C and 6D).

Collectively, these observations support the proposal that S-HDLs are the major HDL species promoting both ABCA1 and macrophage CEC.

DISCUSSION

To investigate the mechanisms that regulate the ability of HDL to promote cholesterol efflux by the ABCA1 pathway, we quantified the CEC of 4 different sizes of r-HDLs. As with human HDL,[7,8] the smallest r-HDL particles were the strongest promoters of cholesterol efflux. Chemical cross-linking followed by MS/MS analysis showed that twice as many intramolecular cross-linked peptides had formed in the smallest r-HDL than in the 3 larger sizes, indicating that apoA1 had markedly higher mobility. When we plotted the positions of the chemically cross-linked peptides on an HDL contact map, virtually all the peptides detected in the 2 largest r-HDL particles were consistent with MD simulations of the double-belt model of apoA1. In this model, the helical repeats of 2 apoA1 molecules assume an antiparallel helical structure that forms a bundle surrounding the edges of discoidal HDL. Because the helical bundle is amphipathic and has high lipid affinity,[42] these observations strongly suggest that most of the apoA1 in the 2 largest HDL particles is bound to lipid and therefore would not be accessible to ABCA1.

The 2 smallest HDL particles showed a different pattern of chemically cross-linked peptides: the peptides of the central region of apoA1 were consistent with the double-belt model, but those at the C-terminus were not (ie, the C-termini in the apoA1 dimer are not in a helical bundle). Moreover, the smallest HDL had the largest number of detectable chemically cross-linked peptides in the C-terminus of apoA1. Taken together, these data indicate that the C-termini of apoA1 in the S-HDL particles have enhanced conformational mobility, likely because of a loss of overall helicity. Because lipid interaction is a major driver of helical formation in apoA1, it is conceivable that the C-terminus is detached from the lipid surface in the 2 smallest r-HDLs as observed in the MD simulations of those particles.

The C-terminus of apoA1 plays a critical role in promoting cholesterol export by ABCA1.[42–44] We envision 2 factors that drive its increased mobility and loss of helical structure in S-HDLs. First, there is crowding. The limited surface area of S-HDL might not accommodate all of the helices of apoA1, preventing the C-termini of apoA1 from lying on the surface of the particle. Second, extreme surface curvature could prevent the C-terminal domain of apoA1 from fully interacting with the lipid because it cannot turn sharply enough to lie down on the surface. In this model,

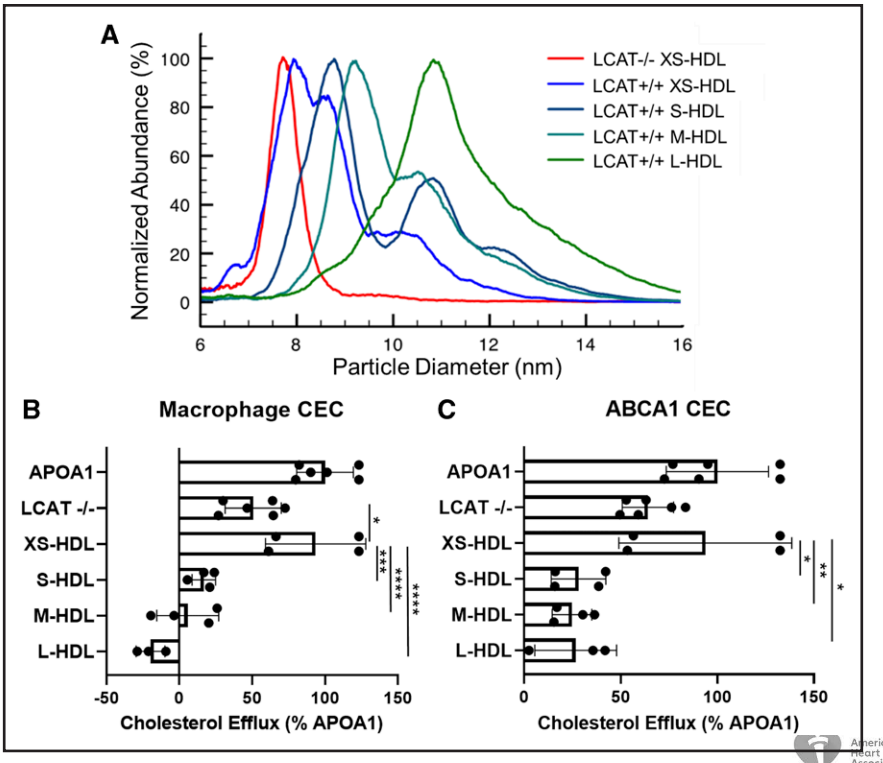

Figure 5. Calibrated IMA (A) and CEC (B) of HDL isolated from plasma of LCAT-deficient (LCAT-/-) and control (XS-HDL, S-HDL, M-HDL, and L-HDL) subjects.

A, Representative IMA size profiles of isolated HDL. To facilitate comparison of size distributions of the particles, the height of each isolated HDL fraction was set to 100%. The diameters of the isolated HDLs of LCAT-/- subjects and control subjects were as follows: LCAT-/-, 7.8±0.1 nm; XS-HDL, 8.1±0.2 nm; S-HDL, 8.8±0.1 nm; M-HDL, 9.8±0.2 nm; and L-HDL, 11.1±0.2 nm. Note that isolated XS-HDL is composed of both XS-HDL and S-HDL particles. **B** and **C**, ABCA1-mediated cholesterol efflux capacity (CEC) of HDL isolated from LCAT-/- subjects and control subjects. Macrophage CEC and ABCA1 CEC of were quantified with [^{3}H]cholesterol-labeled J774 macrophages and baby hamster kidney cells after a 4-hour incubation. Expression of ABCA1 was induced with cAMP and mifepristone, respectively. Cholesterol efflux was calculated as the percentage of radiolabel in the medium of the cells divided by the total radioactivity of the medium and cells. CEC was quantified as the difference in cholesterol efflux of cells with and without induced expression of ABCA1. Isolated HDLs were included in the media of the cells at equal particle concentrations. CEC of HDLs was normalized to CEC of cells exposed to 10 µg/mL of apoA1 (apolipoprotein A1). *P* value: 1-way ANOVA with Tukey-Kramer post-tests. ***$P<0.001$, **$P<0.01$, and *$P<0.05$. ABCA1 indicates ATP-binding cassette transporter A1; HDL, high-density lipoprotein; IMA, ion mobility analysis; LCAT, lecithin-cholesterol acyltransferase; L-HDL, large HDL; M-HDL, medium HDL; S-HDL, small HDL; and XS-HDL, extra-small HDL.

the 2 antiparallel C-termini are "flipped" off the surface of smaller HDLs (Figure 7), where their increased mobility and freedom from lipid binding promote their engagement with ABCA1. In contrast, the C-termini of larger HDLs are strongly bound to lipid and unable to interact productively with ABCA1. On a molar basis, the smallest r-HDL and human HDL particles were as efficient at promoting cholesterol efflux by the ABCA1 pathway as was lipid-free apoA1, which is consistent with this model.

We suggest that the smaller, less lipidated HDL particles may not be fully "filled" with lipid and remain effective substrates for ABCA1. At some point between diameters of 80 and 90 Å, the apoA1 C-terminus finds room to associate with the surface of the particle, shutting down additional lipid accumulation by ABCA1 and possibly promoting the release of a more "mature" particle. In this scheme, the apoA1 C-terminus functions as a lipid level switch that defines the maximal size of HDL particles formed by ABCA1.

An alternative hypothesis for the role of the C-terminus of apoA1 in promoting CEC is that it involves binding of the protein to phospholipid-rich domains in the plasma membrane of cells,[45,46] which in turn promotes phospholipid and cholesterol efflux. Consistent with this, deletion of helices H8 to H10 decreases binding to lipid vesicles but has little impact on cross-linking of radiolabeled apoA1 to ABCA1 on cells. However, our recent studies[47] suggest that the lipid affinity of apoA1 plays a role in promoting the movement of phospholipids from the outer leaflet of the plasma membrane into a hydrophobic tunnel in the interior of the extracellular domain of ABCA1.

To test the relevance of our model system studies to human HDL, we used serum HDL and HDL isolated from LCAT-deficient carriers. Like r-HDLs, the latter is discoidal and composed of apoA1, free cholesterol, and phospholipid. We found that total HDL particle concentration was markedly lower in subjects who completely lacked LCAT activity. The major HDL subspecies in those

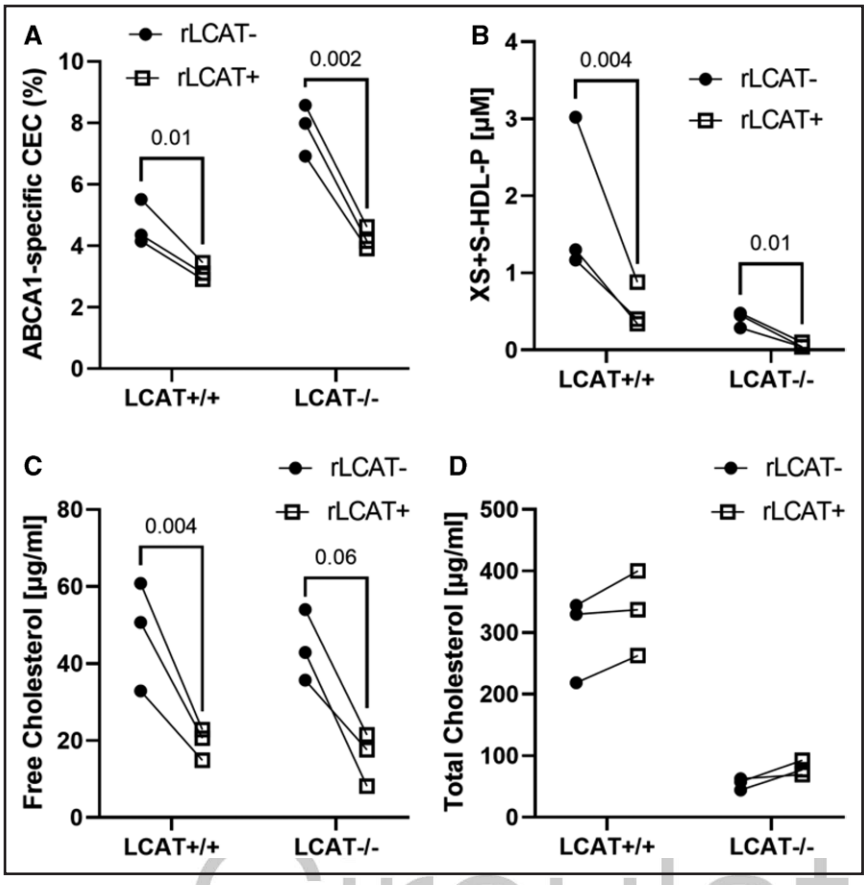

Figure 6. ABCA1 CEC (A), HDL particle size distribution (B), free cholesterol (C), and total cholesterol (D) content of control and LCAT-deficient plasma incubated with LCAT. Control plasma (n=3) and LCAT-deficient plasma (n=3) were incubated with and without recombinant human LCAT (rLCAT+ and rLCAT-; 50 μg/mL) for 1 h at 37 °C. The LCAT reaction was stopped with 2 mM of DTNB and cooling on ice. Control studies demonstrated that DTNB did not alter the CEC of plasma. DTNB was omitted from plasma used to quantify cholesterol levels because it interfered with the enzymatic assay. ABCA1 CEC of plasma was quantified using [^{3}H] cholesterol-labeled baby hamster kidney cells as described in the legend to Figure 5. *P* values, ratio *t* test. ABCA1 indicates ATP-binding cassette transporter A1; CEC, cholesterol efflux capacity; HDL, high-density lipoprotein; HDL-P, HDL particle concentration determined by calibrated ion mobility analysis; LCAT, lecithin-cholesterol acyltransferase; S-HDL, small HDL; and XS-HDL, extra-small HDL.

subjects was XS-HDL, which is very similar in size (78 Å in diameter) to the smallest r-HDL-80 particles used in our model system studies (80 Å). In subjects who were only partially LCAT-deficient, the major HDL subspecies were XS-HDL and S-HDL. In subjects with normal LCAT activity, we detected all 4 sizes of HDL; M-HDL was the major species. Although serum from the LCAT-deficient subjects had very low HDL particle concentrations, ABCA1 CEC and macrophage CEC were similar to that of the controls, strongly suggesting that the ABCA1-specific activities of XS-HDL and S-HDL were greater than those of the larger HDL particles. Consistent with this proposal, macrophage and ABCA1 CEC strongly and positively correlated with the concentration of XS-HDL in plasma.

To confirm these ideas, we used isolated HDL from subjects with and without complete LCAT deficiency. Then we determined macrophage and ABCA1 CEC activity at equal particle concentrations. The isolated particles had diameters of 8.4 nm, 8.8 nm, 9.2 nm, and 14 nm—very similar to the sizes of XS-HDL, S-HDL, M-HDL, and L-HDL in plasma as quantified by calibrated IMA. It is important to note that the isolated HDLs did not precisely mimic the size distributions of the HDL subclasses in plasma from the LCAT-deficient and control subjects. XS-HDL isolated from control subjects, which was a mixture of XS-HDL and S-HDL, had the highest macrophage and ABCA1 CEC–specific activities; they were about 4- to 5-fold greater than those of the 3 larger sizes of isolated HDL. XS-HDL isolated from the LCAT-deficient subjects did not contain S-HDL and was less active than XS-HDL isolated from the control subjects; macrophage CEC and ABCA1 CEC of the isolated HDLs were ~3-fold greater than for the larger sizes of HDL. Lipid-free apoA1 was not detectable in the HDL used for these studies because the particles were isolated by both ultracentrifugation and high-resolution size exclusion chromatography.

These data suggest that both XS-HDL and S-HDL are the major contributors to macrophage and ABCA1 CEC. This hypothesis is strongly supported by the demonstration that incubating control plasma and LCAT-deficient plasma with LCAT converted S-HDLs into L-HDLs and markedly diminished ABCA1 CEC. These observations are remarkably concordant with animal studies, which demonstrated that ABCA1 CEC of plasma HDL was increased in LCAT-/- and LCAT+/- mice.[16] Moreover, overexpression of LCAT significantly reduced macrophage cholesterol efflux by plasma. Taken together, these observations suggest that XS-HDL and S-HDL, which typically represent 20% to 30% of total HDL, are key mediators of ABCA1 CEC and perhaps cardioprotection.

CSL-112, a r-HDL particle that promotes the formation of small and lipid-poor apoA1 particles,[18,19] is being tested in a large, randomized study to determine

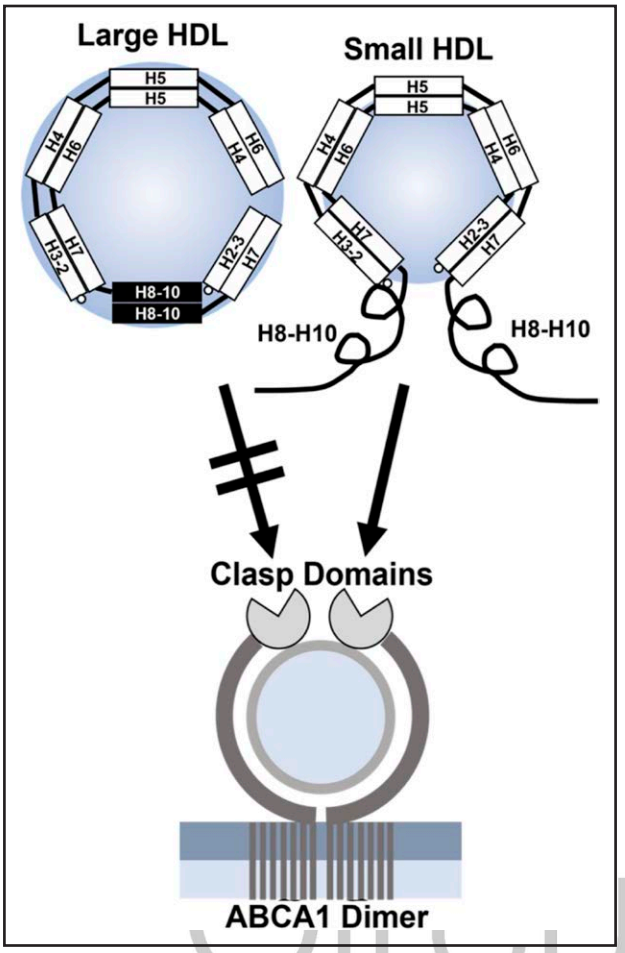

Figure 7. The "flipped ends" model for the increased ABCA1 activity of small HDLs.
In large HDL particles, the C-termini of the apoA1 dimer are in antiparallel helical bundles that are amphipathic and strongly associated with lipid. In small HDL particles, the reduced surface area and high surface curvature force the C-termini off the particles, increasing their mobility. The termini also are less lipid-associated because apoA1 loses its amphipathic double-belt structure. Decreased lipid association and increased mobility of the C-termini (helices H8–H10) promote the engagement of apoA1 with the clasp domains of ABCA1, stimulating cholesterol export from the cell. An alternative hypothesis is that the C-termini of apoA1 promote microsolubilization of phospholipids and cholesterol from phospholipid-rich domains in the plasma membrane of cells (see Discussion). ABCA1 indicates ATP-binding cassette transporter A1; apoA1, apolipoprotein A1; and HDL, high-density lipoprotein.

if it reduces the risk of CVD events in patients after myocardial infarction. The demonstration that CLS-112 lowers incident CVD would strongly support the proposal that S-HDLs are critical in cardioprotection in humans.

Our demonstration that S-HDL and XS-HDL particles potently promote cholesterol efflux from macrophages raises the possibility that increased LCAT activity, which converts smaller HDL particles into larger, cholesteryl ester–rich particles, is a risk factor for atherosclerosis.[48] Consistent with this suggestion, overexpression of LCAT in mice failed to increase reverse cholesterol transport from macrophages to bile.[16] Serum HDL from mice that overexpressed LCAT were less able to promote cholesterol efflux from macrophages by the ABCA1 pathway than control mice.[16] However, studies of the relationships of LCAT to CVD risk in humans have yielded mixed results.[49,50]

One limitation of our investigations is the small number of subjects in our study of LCAT deficiency. However, the large differences in the concentrations of the various sizes of HDL in the different groups of subjects and the consistency of the results with serum HDL and isolated HDL strongly support the proposal that XS-HDL and S-HDL promote cholesterol efflux from macrophages by the ABCA1 pathway. Another limitation is that the size distributions of the isolated HDLs overlapped to some degree, reflecting the limited resolution of size-exclusion chromatography. Nonetheless, the mean sizes of the isolated HDLs were well-separated, and the particle distributions were clearly distinct from one another.

In summary, both our experiments and MD simulations support the proposal that S-HDL particles are potent ligands for promoting cholesterol efflux from macrophages by the ABCA1 pathway. In future studies, it will clearly be important to determine whether XS-HDL and S-HDL predict CVD risk in humans, if LCAT mass or activity associates with HDL size, and if risk prediction is independent of HDL-C.

ARTICLE INFORMATION

Received June 13, 2023; accepted November 5, 2023.

Affiliations

Department of Medicine, University of Washington, Seattle (Y.H., P.M.H., C.T., T.V., K.E.B., J.W.H.). Centro Grossi Paoletti, Dipartimento di Scienze Farmacologiche e Biomolecolari, Università degli Studi di Milano, Italy (C.P., L.C.). Laboratory of Computational Biology, National Heart, Lung, and Blood Institute (M.P., R.W.P.), Department of Laboratory Medicine (A.T.R.), National Institutes of Health, Bethesda, MD. Department of Medicine, Vanderbilt University Medical Center, Nashville, TN (H.D.S., J.P.S.). Department of Medicine, New York University, New York, NY (I.J.G.). Department of Epidemiology, University of Pittsburgh, PA (T.C.). Department of Pathology and Laboratory Medicine, University of Cincinnati College of Medicine, OH (W.S.D.).

Acknowledgments

We thank the Proteomics Resource (UWPR95794, University of Washington) for technical support and Dr Fabrizio Veglia for statistical advice. MD simulations were performed at the National Institutes of Health, Bethesda, MD (BIOWULF and Lobos clusters), and on the Anton2 supercomputer. Access to Anton 2 was generously provided by D.E. Shaw Research.

Sources of Funding

This work was supported by awards from the National Institutes of Health: T32HL007828, R01HL149685, R35HL150754, P01HL151328, P01HL128203, P30DK017047, R01HL153118, R01HL155601, R01HL144558, and R01HL149685; the American Heart Association (15POST22700033); and the Intramural Program of the National Heart, Lung, and Blood Institute of the National Institutes of Health. Anton 2 time was provided by the Pittsburgh Supercomputing Center (National Institutes of Health, R01GM116961).

Disclosures

K.E.B. serves on the Scientific Advisory Board of Esperion Therapeutics. The other authors report no conflicts.

Supplemental Material

Expanded Methods
Figures S1–S3
Tables S1–S3

REFERENCES

1. Gordon DJ, Rifkind BM. High-density lipoprotein--the clinical implications of recent studies. *N Engl J Med*. 1989;321:1311–1316. doi: 10.1056/NEJM198911093211907
2. Rader DJ, Hovingh GK. HDL and cardiovascular disease. *Lancet*. 2014;384:618–625. doi: 10.1016/S0140-6736(14)61217-4
3. Rader DJ, Tall AR. The not-so-simple HDL story: is it time to revise the HDL cholesterol hypothesis? *Nat Med*. 2012;18:1344–1346. doi: 10.1038/nm.2937
4. Heinecke J. HDL and cardiovascular-disease risk--time for a new approach? *N Engl J Med*. 2011;364:170–171. doi: 10.1056/NEJMe1012520
5. Rader DJ, Alexander ET, Weibel GL, Billheimer J, Rothblat GH. The role of reverse cholesterol transport in animals and humans and relationship to atherosclerosis. *J Lipid Res*. 2009;50(suppl):S189–S194. doi: 10.1194/jlr.R800088-JLR200
6. Oram JF, Heinecke JW. ATP-binding cassette transporter A1: a cell cholesterol exporter that protects against cardiovascular disease. *Physiol Rev*. 2005;85:1343–1372. doi: 10.1152/physrev.00005.2005
7. Du XM, Kim MJ, Hou L, Le Goff W, Chapman MJ, Van Eck M, Curtiss LK, Burnett JR, Cartland SP, Quinn CM, et al. HDL particle size is a critical determinant of ABCA1-mediated macrophage cellular cholesterol export. *Circ Res*. 2015;116:1133–1142. doi: 10.1161/CIRCRESAHA.116.305485
8. He Y, Ronsein GE, Tang C, Jarvik GP, Davidson WS, Kothari V, Song HD, Segrest JP, Bornfeldt KE, Heinecke JW. Diabetes impairs cellular cholesterol efflux from ABCA1 to small HDL particles. *Circ Res*. 2020;127:1198–1210. doi: 10.1161/CIRCRESAHA.120.317178
9. Yvan-Charvet L, Wang N, Tall AR. Role of HDL, ABCA1, and ABCG1 transporters in cholesterol efflux and immune responses. *Arterioscler Thromb Vasc Biol*. 2010;30:139–143. doi: 10.1161/ATVBAHA.108.179283
10. de la Llera-Moya M, Drazul-Schrader D, Asztalos BF, Cuchel M, Rader DJ, Rothblat GH. The ability to promote efflux via ABCA1 determines the capacity of serum specimens with similar high-density lipoprotein cholesterol to remove cholesterol from macrophages. *Arterioscler Thromb Vasc Biol*. 2010;30:796–801. doi: 10.1161/ATVBAHA.109.199158
11. Khera AV, Cuchel M, de la Llera-Moya M, Rodrigues A, Burke MF, Jafri K, French BC, Phillips JA, Mucksavage ML, Wilensky RL, et al. Cholesterol efflux capacity, high-density lipoprotein function, and atherosclerosis. *N Engl J Med*. 2011;364:127–135. doi: 10.1056/NEJMoa1001689
12. Rohatgi A, Khera A, Berry JD, Givens EG, Ayers CR, Wedin KE, Neeland IJ, Yuhanna IS, Rader DR, de Lemos JA, et al. HDL cholesterol efflux capacity and incident cardiovascular events. *N Engl J Med*. 2014;371:2383–2393. doi: 10.1056/NEJMoa1409065
13. Saleheen D, Scott R, Javad S, Zhao W, Rodrigues A, Picataggi A, Lukmanova D, Mucksavage ML, Luben R, Billheimer J, et al. Association of HDL cholesterol efflux capacity with incident coronary heart disease events: a prospective case-control study. *Lancet Diabetes Endocrinol*. 2015;3:507–513. doi: 10.1016/S2213-8587(15)00126-6
14. Kunnen S, Van Eck M. Lecithin:cholesterol acyltransferase: old friend or foe in atherosclerosis? *J Lipid Res*. 2012;53:1783–1799. doi: 10.1194/jlr.R024513
15. Berard AM, Foger B, Remaley A, Shamburek R, Vaisman BL, Talley G, Paigen B, Hoyt RF Jr, Marcovina S, Brewer HB Jr, et al. High plasma HDL concentrations associated with enhanced atherosclerosis in transgenic mice overexpressing lecithin-cholesteryl acyltransferase. *Nat Med*. 1997;3:744–749. doi: 10.1038/nm0797-744
16. Tanigawa H, Billheimer JT, Tohyama J, Fuki IV, Ng DS, Rothblat GH, Rader DJ. Lecithin: cholesterol acyltransferase expression has minimal effects on macrophage reverse cholesterol transport in vivo. *Circulation*. 2009;120:160–169. doi: 10.1161/CIRCULATIONAHA.108.825109
17. Calabresi L, Baldassarre D, Castelnuovo S, Conca P, Bocchi L, Candini C, Frigerio B, Amato M, Sirtori CR, Alessandrini P, et al. Functional lecithin: cholesterol acyltransferase is not required for efficient atheroprotection in humans. *Circulation*. 2009;120:628–635. doi: 10.1161/CIRCULATIONAHA.108.818143
18. Kingwell BA, Nicholls SJ, Velkoska E, Didichenko SA, Duffy D, Korjian S, Gibson CM. Antiatherosclerotic effects of CSL112 mediated by enhanced cholesterol efflux capacity. *J Am Heart Assoc*. 2022;11:e024754. doi: 10.1161/JAHA.121.024754
19. Didichenko SA, Navdaev AV, Cukier AM, Gille A, Schuetz P, Spycher MO, Therond P, Chapman MJ, Kontush A, Wright SD. Enhanced HDL functionality in small HDL species produced upon remodeling of HDL by reconstituted HDL, CSL112: effects on cholesterol efflux, anti-inflammatory and antioxidative activity. *Circ Res*. 2016;119:751–763. doi: 10.1161/CIRCRESAHA.116.308685
20. He Y, Song HD, Anantharamaiah GM, Palgunachari MN, Bornfeldt KE, Segrest JP, Heinecke JW. Apolipoprotein A1 forms 5/5 and 5/4 antiparallel dimers in human high-density lipoprotein. *Mol Cell Proteomics*. 2019;18:854–864. doi: 10.1074/mcp.RA118.000878
21. Tubb MR, Smith LE, Davidson WS. Purification of recombinant apolipoproteins A-I and A-IV and efficient affinity tag cleavage by tobacco etch virus protease. *J Lipid Res*. 2009;50:1497–1504. doi: 10.1194/jlr.D900003-JLR200
22. Cavigiolio G, Shao B, Geier EG, Ren G, Heinecke JW, Oda MN. The interplay between size, morphology, stability, and functionality of high-density lipoprotein subclasses. *Biochemistry*. 2008;47:4770–4779. doi: 10.1021/bi7023354
23. Hutchins PM, Ronsein GE, Monette JS, Pamir N, Wimberger J, He Y, Anantharamaiah GM, Kim DS, Ranchalis JE, Jarvik GP, et al. Quantification of HDL particle concentration by calibrated ion mobility analysis. *Clin Chem*. 2014;60:1393–1401. doi: 10.1373/clinchem.2014.228114
24. Caulfield MP, Li S, Lee G, Blanche PJ, Salameh WA, Benner WH, Reitz RE, Krauss RM. Direct determination of lipoprotein particle sizes and concentrations by ion mobility analysis. *Clin Chem*. 2008;54:1307–1316. doi: 10.1373/clinchem.2007.100586
25. Guha S, Li M, Tarlov MJ, Zachariah MR. Electrospray-differential mobility analysis of bionanoparticles. *Trends Biotechnol*. 2012;30:291–300. doi: 10.1016/j.tibtech.2012.02.003
26. Rinner O, Seebacher J, Walzthoeni T, Mueller LN, Beck M, Schmidt A, Mueller M, Aebersold R. Identification of cross-linked peptides from large sequence databases. *Nat Methods*. 2008;5:315–318. doi: 10.1038/nmeth.1192
27. Pourmousa M, Song HD, He Y, Heinecke JW, Segrest JP, Pastor RW. Tertiary structure of apolipoprotein A-I in nascent high-density lipoproteins. *Proc Natl Acad Sci U S A*. 2018;115:5163–5168. doi: 10.1073/pnas.1721181115
28. Pan AC, Weinreich TM, Piana S, Shaw DE. Demonstrating an order-of-magnitude sampling enhancement in molecular dynamics simulations of complex protein systems. *J Chem Theory Comput*. 2016;12:1360–1367. doi: 10.1021/acs.jctc.5b00913
29. Jo S, Kim T, Iyer VG, Im W. CHARMM-GUI: a web-based graphical user interface for CHARMM. *J Comput Chem*. 2008;29:1859–1865. doi: 10.1002/jcc.20945
30. Jones MK, Gu F, Catte A, Li L, Segrest JP. "Sticky" and "promiscuous," the yin and yang of apolipoprotein A-I termini in discoidal high-density lipoproteins: a combined computational-experimental approach. *Biochemistry*. 2011;50:2249–2263. doi: 10.1021/bi101301g
31. Calabresi L, Pisciotta L, Costantin A, Frigerio I, Eberini I, Alessandrini P, Arca M, Bon GB, Boscutti G, Busnach G, et al. The molecular basis of lecithin:cholesterol acyltransferase deficiency syndromes: a comprehensive study of molecular and biochemical findings in 13 unrelated Italian families. *Arterioscler Thromb Vasc Biol*. 2005;25:1972–1978. doi: 10.1161/01.ATV.0000175751.30616.13
32. George RT, Abuhatzira L, Stoughton SM, Karathanasis SK, She D, Jin C, Buss N, Bakker-Arkema R, Ongstad EL, Koren M, et al. MEDI6012: recombinant human lecithin cholesterol acyltransferase, high-density lipoprotein, and low-density lipoprotein receptor-mediated reverse cholesterol transport. *J Am Heart Assoc*. 2021;10:e014572. doi: 10.1161/JAHA.119.014572
33. Mendez AJ, Oram JF, Bierman EL. Protein kinase C as a mediator of high density lipoprotein receptor-dependent efflux of intracellular cholesterol. *J Biol Chem*. 1991;266:10104–10111.
34. Segrest JP, Jones MK, Klon AE, Sheldahl CJ, Hellinger M, De Loof H, Harvey SC. A detailed molecular belt model for apolipoprotein A-I in discoidal high density lipoprotein. *J Biol Chem*. 1999;274:31755–31758. doi: 10.1074/jbc.274.45.31755
35. Mei X, Atkinson D. Crystal structure of C-terminal truncated apolipoprotein A-I reveals the assembly of high density lipoprotein (HDL) by dimerization. *J Biol Chem*. 2011;286:38570–38582. doi: 10.1074/jbc.M111.260422
36. Davidson WS, Thompson TB. The structure of apolipoprotein A-I in high density lipoproteins. *J Biol Chem*. 2007;282:22249–22253. doi: 10.1074/jbc.R700014200
37. Thomas MJ, Bhat S, Sorci-Thomas MG. Three-dimensional models of HDL apoA-I: implications for its assembly and function. *J Lipid Res*. 2008;49:1875–1883. doi: 10.1194/jlr.R800010-JLR200
38. Lima DB, Melchior JT, Morris J, Barbosa VC, Chamot-Rooke J, Fioramonte M, Souza T, Fischer JSG, Gozzo FC, Carvalho PC, et al. Characterization of homodimer interfaces with cross-linking mass

spectrometry and isotopically labeled proteins. *Nat Protoc*. 2018;13:431–458. doi: 10.1038/nprot.2017.113
39. Forte T, Norum KR, Glomset JA, Nichols AV. Plasma lipoproteins in familial lecithin: cholesterol acyltransferase deficiency: structure of low and high density lipoproteins as revealed by electron microscopy. *J Clin Invest*. 1971;50:1141–1148. doi: 10.1172/JCI106586
40. Asztalos BF, Schaefer EJ, Horvath KV, Yamashita S, Miller M, Franceschini G, Calabresi L. Role of LCAT in HDL remodeling: investigation of LCAT deficiency states. *J Lipid Res*. 2007;48:592–599. doi: 10.1194/jlr.M600403-JLR200
41. Rosenson RS, Brewer HB Jr, Chapman MJ, Fazio S, Hussain MM, Kontush A, Krauss RM, Otvos JD, Remaley AT, Schaefer EJ. HDL measures, particle heterogeneity, proposed nomenclature, and relation to atherosclerotic cardiovascular events. *Clin Chem*. 2011;57:392–410. doi: 10.1373/clinchem.2010.155333
42. Segrest JP, Jones MK, De Loof H, Brouillette CG, Venkatachalapathi YV, Anantharamaiah GM. The amphipathic helix in the exchangeable apolipoproteins: a review of secondary structure and function. *J Lipid Res*. 1992;33:141–166.
43. Shao B, Fu X, McDonald TO, Green PS, Uchida K, O'Brien KD, Oram JF, Heinecke JW. Acrolein impairs ATP binding cassette transporter A1-dependent cholesterol export from cells through site-specific modification of apolipoprotein A-I. *J Biol Chem*. 2005;280:36386–36396. doi: 10.1074/jbc.M508169200
44. Mei X, Liu M, Herscovitz H, Atkinson D. Probing the C-terminal domain of lipid-free apoA-I demonstrates the vital role of the H10B sequence repeat in HDL formation. *J Lipid Res*. 2016;57:1507–1517. doi: 10.1194/jlr.M068874
45. Vedhachalam C, Ghering AB, Davidson WS, Lund-Katz S, Rothblat GH, Phillips MC. ABCA1-induced cell surface binding sites for ApoA-I. *Arterioscler Thromb Vasc Biol*. 2007;27:1603–1609. doi: 10.1161/ATVBAHA.107.145789
46. Phillips MC. Is ABCA1 a lipid transfer protein? *J Lipid Res*. 2018;59:749–763. doi: 10.1194/jlr.R082313
47. Segrest JP, Tang C, Song HD, Jones MK, Davidson WS, Aller SG, Heinecke JW. ABCA1 is an extracellular phospholipid translocase. *Nat Commun*. 2022;13:4812. doi: 10.1038/s41467-022-32437-3
48. Heinecke JW. Small HDL promotes cholesterol efflux by the ABCA1 pathway in macrophages: implications for therapies targeted to HDL. *Circ Res*. 2015;116:1101–1103. doi: 10.1161/CIRCRESAHA.115.306052
49. Holleboom AG, Kuivenhoven JA, Vergeer M, Hovingh GK, van Miert JN, Wareham NJ, Kastelein JJ, Khaw KT, Boekholdt SM. Plasma levels of lecithin:cholesterol acyltransferase and risk of future coronary artery disease in apparently healthy men and women: a prospective case-control analysis nested in the EPIC-Norfolk population study. *J Lipid Res*. 2010;51:416–421. doi: 10.1194/P900038-JLR200
50. Dullaart RP, Perton F, van der Klauw MM, Hillege HL, Sluiter WJ; PREVEND Study Group. High plasma lecithin:cholesterol acyltransferase activity does not predict low incidence of cardiovascular events: possible attenuation of cardioprotection associated with high HDL cholesterol. *Atherosclerosis*. 2010;208:537–542. doi: 10.1016/j.atherosclerosis.2009.07.042